

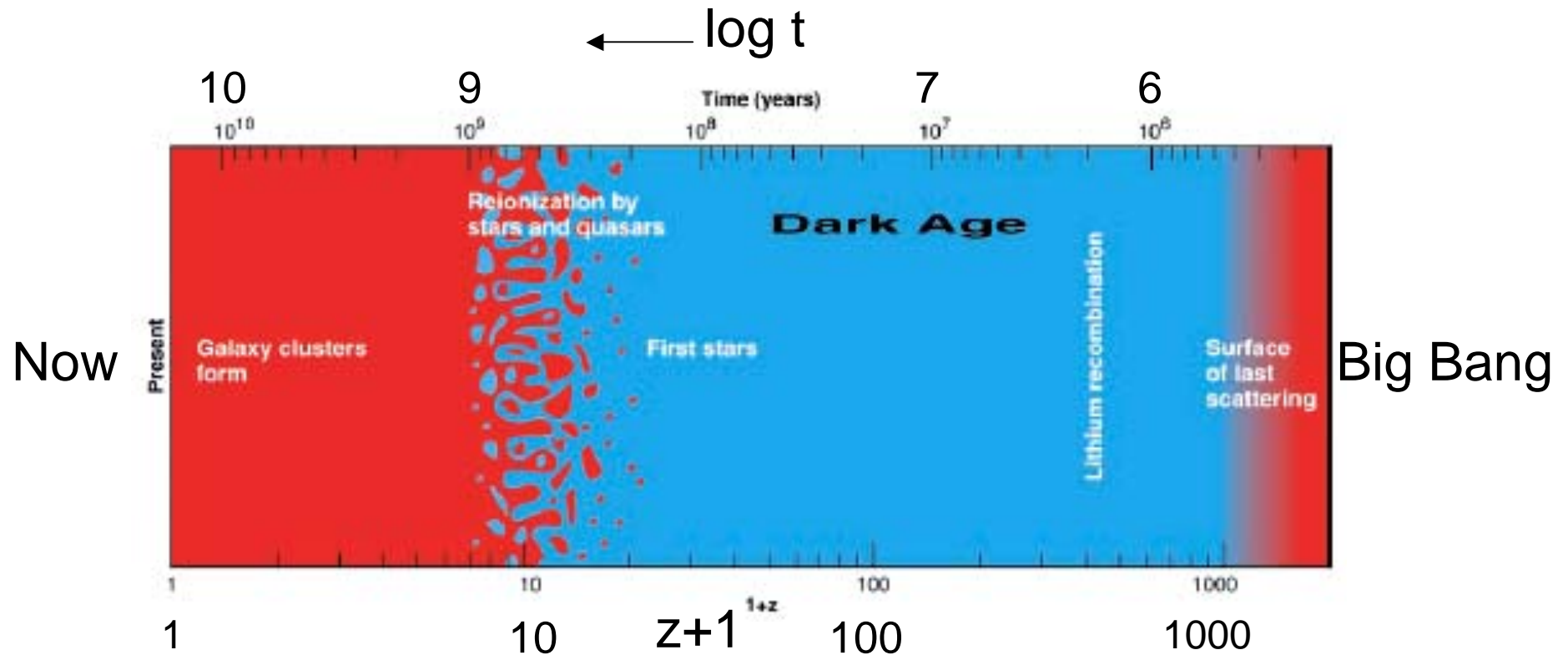
# Lecture 27 – The Intergalactic Medium

1. Cosmological Scenario
2. The Ly $\alpha$  Forest
3. Ionization of the Forest
4. The Gunn-Peterson Effect
5. Comment on Hell Reionization

## References

J Miralda-Escude', Science 300 1904 2003  
M Rauch, ARAA 36 267 1998  
A Loeb & R Barkana, ARAA 39 19 2001  
X Fan et al. ARAA 44 415 2006  
X Fan AJ 132 117 2006

# 1. Cosmological Scenario



The universe recombined at  $z \sim 1100$  (300,000 yr) and was re-ionized much later (10-20 Gyr) by the radiation from the first stars and galaxies.

J. Miralda-Escudé, Science, 300, 1904 2003

# Cosmological Formulae Redux

## *Concordance Cosmological Parameters*

$$\Omega_i = \frac{\rho_i}{\rho_{cr}} \quad \rho = \rho_{\Lambda} + \rho_{DM} + \rho_B$$

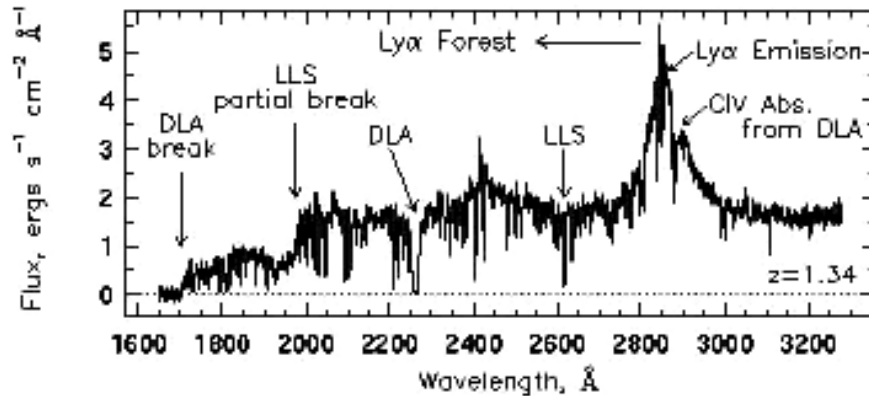
$$\rho_{cr} = \frac{3H_0^2}{8\pi G} = h^2 1.88 \times 10^{-29} \text{ gr cm}^{-3} \quad H_0 = h 100 \text{ km s}^{-1} \text{Mpc}^{-1}$$

$h = 0.70$	$\Omega_{\Lambda} = 0.73$	$\Omega_{DM} = 0.22$	$\Omega_B = 0.04$
------------	---------------------------	----------------------	-------------------

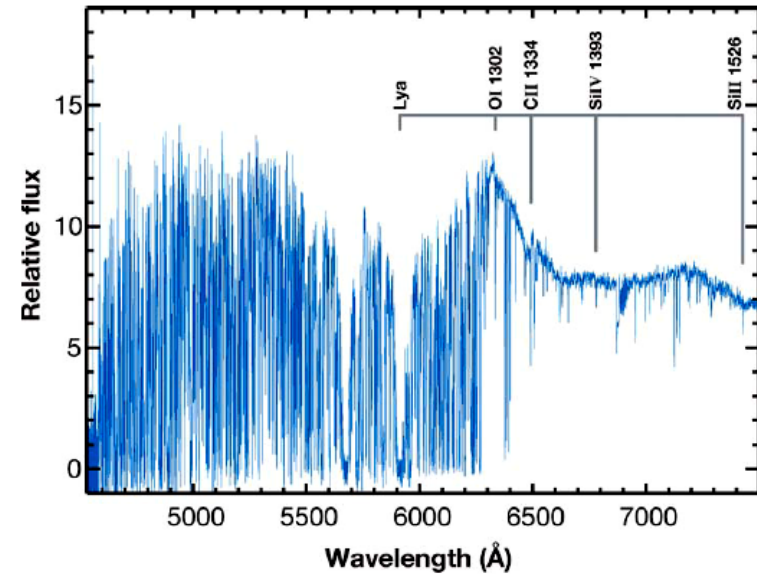
$$\lambda = \lambda_0 (1 + z)$$

$$t = \frac{t_n}{(1 + z)^{3/2}} \quad t_n \cong 13.73 \text{ Gyr}$$

## 2. Lyman- $\alpha$ Forest



PKS 0454+0339,  $z = 1.34$



PSS 0209+0517

1. The huge number of Ly $\alpha$  absorbers dominates the mass of the IGM: If  $\tilde{N}$  is the number distribution function of Ly $\alpha$  clouds and  $N$  is the column density of atomic hydrogen, then  $\tilde{N}(N, z)$  has the following properties:

- $\tilde{N}(z)$  increases rapidly with  $z$ , roughly as  $(1+z)^{2.5}$
- $\tilde{N}(N)$  decreases rapidly with  $N$ , roughly as  $N^{-1.5}$

# More on the Ly $\alpha$ Forest

2. Since Ly $\alpha$  Forest clouds are defined as optically thin to Lyman continuum photons ( $\log N < 17.2$ ), they are ionized, and most of their mass is not detected by Ly $\alpha$  absorption.
3. Upper limits to the temperature come from the modest line widths,  $b_D \sim 20 - 25 \text{ km s}^{-1}$  or  $T \sim 30,000 \text{ K}$ .\*
4. The IGM ionizing radiation field and ionization rate can be estimated from a “proximity effect”, i.e., from the variation in  $\tilde{N}$  near quasars:  
$$J \sim 10^{-21} \text{ erg cm}^{-2} \text{ s}^{-1} \text{ sr}^{-1} \text{ Hz}^{-1} \quad G \sim 10^{-12} \text{ s}^{-1}$$
5. Photoionization-simulation models give  $x(\text{H}) \sim 10^{-5}$ .
6. Flat structures for small columns,  $\sim 50 \text{ kpc}$  thick and  $\sim \text{Mpc}$  wide are suggested by a few lensed quasars and quasar pairs.

\*  $b_D = 22.5 \text{ km/s}$  corresponds to  $\text{FWHM} = 53 \text{ km/s}$

# Comparison with the Diffuse ISM

The Ly- $\alpha$  forest arises from quasi-distinct features, although a smooth background distribution is not ruled out.

Compare the IGM at  $z \sim 3$  with the closest ISM phases\*:

**WIM\***  $n \sim 0.375 \text{ cm}^{-3}$        **$T \sim 8000 \text{ K}$**

**HIM**  $n \sim 0.003 \text{ cm}^{-3}$        **$T \sim 10^6 \text{ K}$**

**IGM ( $z \sim 3$ )**  $n \sim 10^{-5} \text{ cm}^{-3}$        **$T \sim 3 \times 10^4 \text{ K}$**

*The thermal pressure of the IGM is tiny.*

- The ISM gas of the Milky Way is bound by gravity and balanced in hydrostatic equilibrium with several sources of pressures.
- The IGM is governed largely by the gravity of CDM halos plus self-gravity and shocks in a highly clustered medium.

\*The numbers for the WIM refer to its denser parts (Lec08)

### 3. Photoionization Modeling

We provide the elementary basis for these models by considering the physical conditions at a typical location in a uniform and flat cosmological model. Of course, current understanding of the Ly  $\alpha$  forest is based on *non-uniform* structures that arose from primordial fluctuations and evolved dynamically according to the  $\Lambda$ CDM cosmology (with the parameters given earlier).

#### a. Post-recombination Density

$$\rho_B = \rho_H + \rho_{\text{He}} = \rho_H + Y\rho_B$$

$$n_H = (1 - Y) \frac{\rho_B}{m_H} = (1 - Y) \Omega_B \frac{\rho_{cr}}{m_H}$$

$$n_{\text{H}} = (1 - Y) \frac{\rho_{\text{cr}}}{m_{\text{H}}} \Omega_{\text{B}} (1 + z)^3 \cong 1.6 \times 10^{-7} \text{ cm}^{-3} (1 + z)^3$$

e.g., at recombination ( $z \sim 1000$ ):  $n_{\text{H}} \sim 200 \text{ cm}^{-3}$   
 at reionization ( $z \sim 7$ ):  $n_{\text{H}} \sim 10^{-4} \text{ cm}^{-3}$

## b. Local Photoionization Balance

The basic physics was covered in Lec03. The controlling parameter is the ***ionization parameter***, in this case  **$G/n_{\text{H}}\alpha$** . Although surely variable, typical parameters for the IGM might be (see Sec. 3d below):

$$G \sim 10^{-12} \text{ s}^{-1} \quad T \sim 30,000 \text{ K} \quad x(\text{H}) \sim 10^{-5}$$

With  $\alpha \sim 2 \times 10^{-13} \text{ cm}^3 \text{ s}^{-1}$ ,

$$\frac{G}{n\alpha} = 2.5 \times 10^7 (1 + z)^{-3} \gg 1 \quad \text{for } z \leq 10$$



This large value means that ***the photoionization time is much shorter than the recombination time***,

$$\tau_{\text{ph}} = \frac{1}{G} \ll \tau_{\text{rec}} = \frac{1}{n_e \alpha}$$

and implies that ***the IGM is fully ionized***:  $n_e = n_{\text{H}}$ .

### c. Atomic Hydrogen Abundance

The chemical balance equations are:

$$\alpha(\text{H}^+) n_e n(\text{H}^+) = G(\text{H}) n(\text{H})$$

$$n_{\text{H}} = n(\text{H}^+) + n(\text{H}) \quad n_e = n(\text{H}^+) + N(\text{He}^+) + n(\text{He}^{++})$$

Again using  $n_e = n_{\text{H}}$ , the abundance of H is:

$$x(\text{H}) = \left( 1 + \frac{G}{n_{\text{H}} \alpha} \right)^{-1} \approx \left( \frac{G}{n_{\text{H}} \alpha} \right)^{-1} = 4 \times 10^{-8} (1+z)^3 \ll 1$$

#### d. The Ionization Flux of a Quasar

The IGM radiation field is clearly basic for understanding the Ly- $\alpha$  forest. It depends on cosmic time through the history of star, galaxy, and quasar formation. We give just one estimate, that due to a luminous quasar, analogous to those made for O & B stars in earlier lectures. For further discussion, see Loeb & Barkana, ARAA 39 19 2001.

$$G = \int_{\nu_1}^{\infty} d\nu \frac{4\pi J_{\nu}}{h\nu} \sigma_1(\nu) \quad \sigma_1(\nu) = \sigma_1(\nu_1) \left(\frac{\nu_1}{\nu}\right)^3$$

We use an empirical SED for quasars (Madau astro-ph 0005106 2001) with  $\nu_1$  the frequency at the Lyman edge

$$L_{\nu} \cong L_1 \left(\frac{\nu_1}{\nu}\right)^2 \quad L_1 = 10^{30} \text{ erg s}^{-1} \text{ Hz}^{-1} \quad 4\pi J_{\nu} \approx \frac{L_{\nu}}{4\pi r^2}$$

The result for the ionization rate at Mpc distances is

$$G = 2 \times 10^{-12} \text{ s}^{-1} \frac{L}{L_1} \left( \frac{\text{Mpc}}{r} \right)^2$$

This is the same order of magnitude found in simulations (where  $G$  is assumed to be same everywhere).

The problem is complicated because one has to include the contributions of all relevant quasars, especially those close to the line of sight and also do the radiative transfer.

As for H II regions, one can evaluate the heating rate, or equivalently the mean photo-electron energy, as,

$$\bar{E}_2 = \frac{\int_{\nu_1}^{\infty} h(\nu - \nu_1) \sigma_{\nu} \frac{4\pi J_{\nu}}{h\nu} d\nu}{\int_{\nu_1}^{\infty} \sigma_{\nu} \frac{4\pi J_{\nu}}{h\nu} d\nu}$$

## 4. Gunn Peterson Effect

Almost immediately after the discovery of quasars, Gunn and Peterson (ApJ 142 1633 1965) considered the effect of a *distribution of intervening atomic H* on quasar spectra arising from the “resonant scattering” of Ly $\alpha$  photons of the quasar continuum (shortward of Ly $\alpha$ ). Resonant scattering is closely related to the photo-absorption process responsible for the absorption lines; it refers to the photon emitted following absorption:

$$h\nu + H(n = 1) \rightarrow H(n = 2) \rightarrow H(n = 1) + h\nu'$$

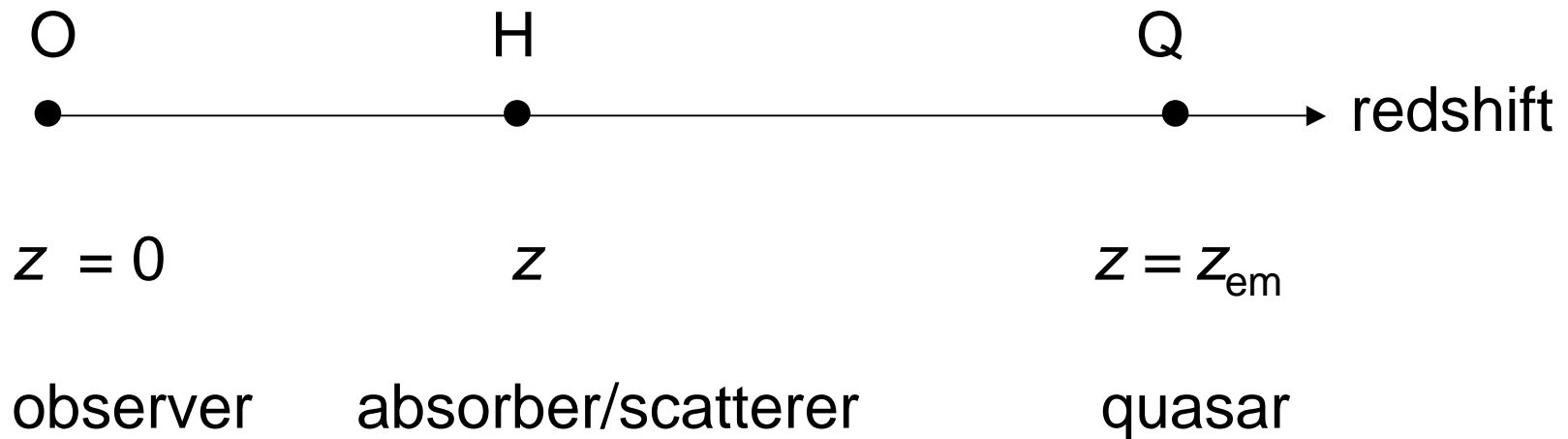
---

In the following diagram of the GP effect,

$\lambda(Q)$  = wavelength of the photon absorbed at redshift  $z$

$\lambda(O)$  = the observed wavelength

$\lambda(\text{Ly}\alpha)$  = rest wavelength of the Lyman  $\alpha$  line



The observed and emitted wavelengths satisfy the relations

$$(1+z_{\text{em}})\lambda(Q) = \lambda(O) \quad \text{and} \quad (1+z) \lambda(\text{Ly}\alpha) = \lambda(O)$$

or,

$$\lambda(Q) = \frac{1+z}{1+z_{\text{em}}} \lambda(\text{Ly}\alpha) < \lambda(\text{Ly}\alpha)$$

i.e., the absorbed continuum photon has a wavelength shorter than the Lyman  $\alpha$  line

## GP Optical Depth

Gunn and Peterson (GP) calculate the observed absorption optical depth at frequency  $\nu(O)$  in terms of the optical depth in the emitting frame where  $\nu = (1+z)\nu(O)$  :

$$d\tau = f_{12} \frac{\pi e^2}{m_e c} \varphi[(1+z)\nu(O) - \nu_{12}] n_1(z) dl$$

where  $\varphi$  is the lineshape function and  $\nu_{12} = \nu(\text{Ly}\alpha)$ . Since the range in  $z$  is very much larger than the linewidth, the integration is easily carried out on using

$$\frac{dl}{dz} = \Omega_m \frac{c}{H_0} (1+z)^{-5/2}$$

Setting  $n_1 = n(H)$ , the GP optical depth is

$$\tau_{GP} = f_{12} \lambda_{12} \frac{\pi e^2}{m_e c} n(H) \frac{c}{H_0} (1+z)^{-3/2}$$

**Note the dependence on  $f\lambda$ .**

## Estimate of the GP Optical Depth

Combining this result with the expression for  $n_{\text{H}}$  on slide 8, with  $n(\text{H}) = x(\text{H}) n_{\text{H}}$ , and using the cosmological parameters on slide 3, yields:

$$\tau_{GP} \approx 2.6 \times 10^4 x(\text{H}) (1+z)^{3/2}$$

- Even for a small neutral H fraction  $\sim 10^{-4}$ , the optical depth for  $z \sim 6$  is large. Of course photoionization models show that  $x(\text{H})$  is sensitive to the ionization rate  $G$  (as  $1/G$ );  $\tau_{GP}$  is large from the recombination epoch until re-ionization.
- Although there had been evidence for a finite  $\tau_{GP}$  in the spectra of high- $z$  quasars, truly convincing data only became available from the  $z \sim 6$  quasars found by the Sloan Digital Sky Survey (SDSS).

# Onset of GP Troughs for High- $z$ Quasars

Pre-SDSS Q 1422+23 ( $z_{\text{em}}=3.62$ )  
c.f, Rauch ARAA 36 267 1998

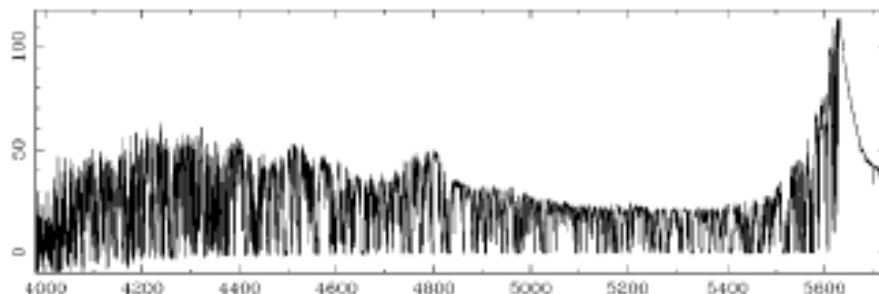


Figure 1 High resolution [full width at half maximum (FWHM)  $\approx 6.6 \text{ km s}^{-1}$ ] spectrum of the  $z_{\text{em}} = 3.62$  QSO1422+23 ( $V = 16.5$ ), taken with the Keck High Resolution Spectrograph (HIRES) (signal-to-noise ratio  $\sim 150$  per resolution element, exposure time 25,000 s). Data from Womble et al (1996).

High red-shift quasar showing rich Ly  $\alpha$  forest plus absorption line systems for Ly  $\beta$ , Si IV, and CIV, but no strong evidence for a GP trough between the lines.

Q 1030+0524 has no detectable flux short of Ly  $\alpha$  & Ly  $\beta$ .

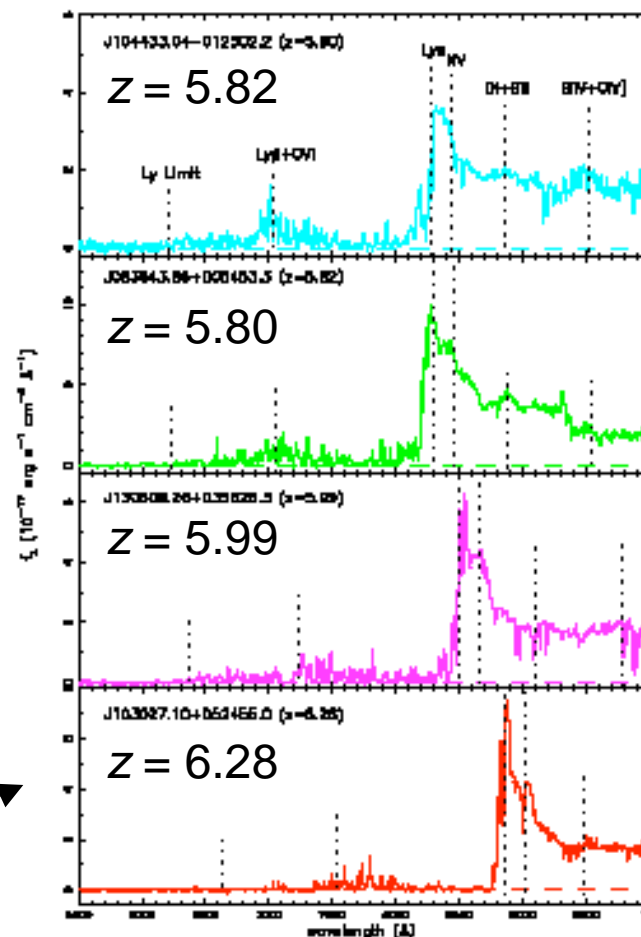


FIG. 2.— Optical spectra of  $z \geq 5.6$  quasars observed with Keck/HIRES, in the observed frame. The spectra have been smoothed to  $4 \text{ \AA pixel}^{-1}$ , and have been normalized to the observed  $z$  band flux. The spectrum of SDSSJ044-0125 has been taken from Fan et al. (2006). In each spectrum, the expected wavelengths of prominent emission lines, as well as the Lyman limit, are indicated by the dashed lines.

**High- $z$  SDSS Quasars, Becker et al., ApJ 122 2850 2001**

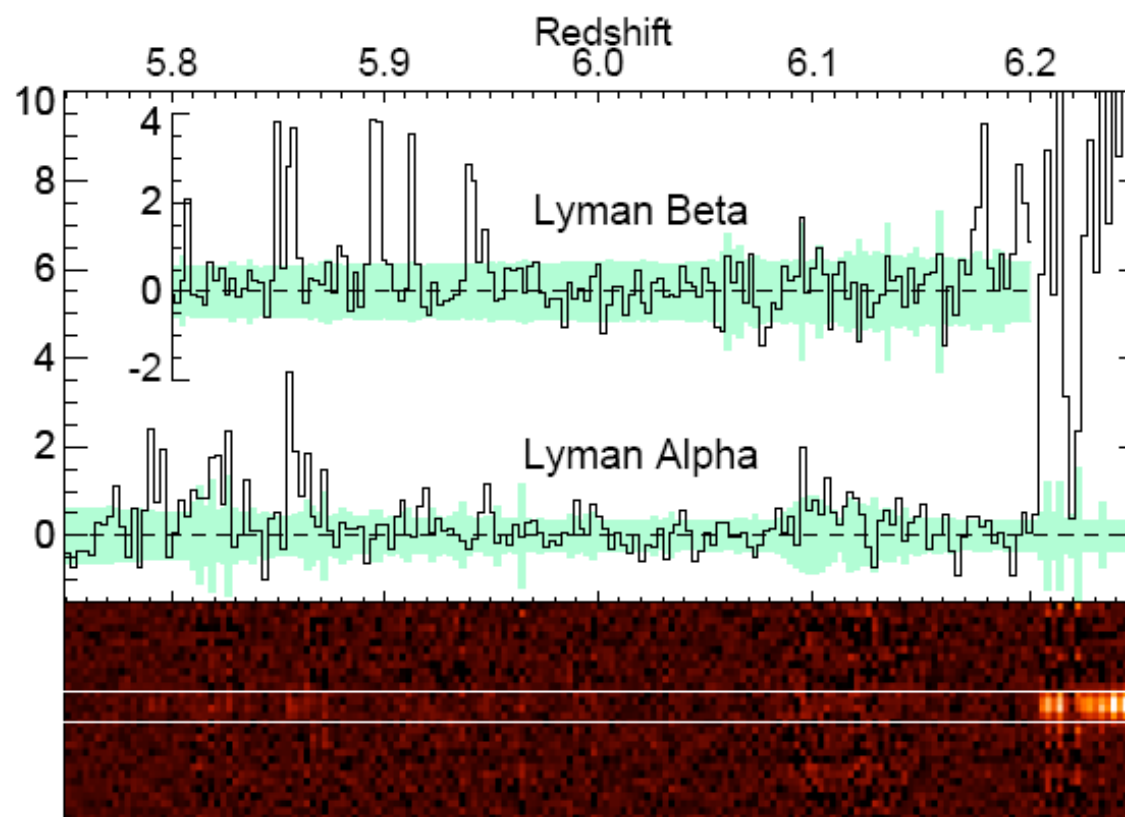


# Close Up of SDSS 1030+0524 ( $z_{\text{em}} = 6.28$ )

Becker et al. (2001)

Keck/ESI Ly  $\beta$   
spectrum  
6920-7440 Å

Keck/ESI Ly  $\alpha$   
spectrum  
8200-8810 Å



$$\tau_{\text{GP}}(\text{Ly}\alpha) > 5 \quad \tau_{\text{GP}}(\text{Ly}\beta) > 20$$

**HI Reionization occurs at  $z \sim 6$  or before**

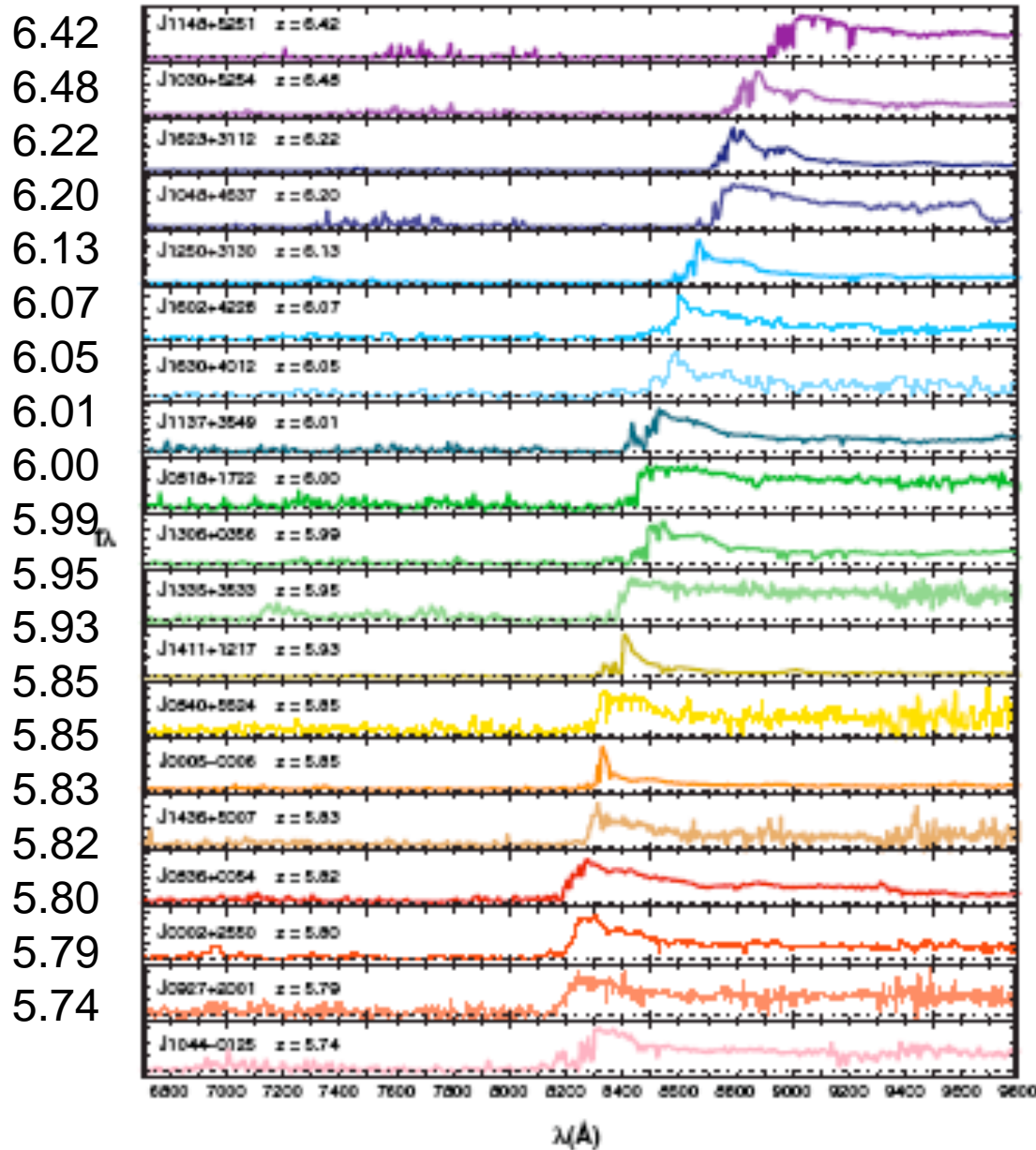
## Ly $\gamma$ & Ly $\beta$ Troughs and Reionization

Since  $\tau_{\text{GP}} \sim f\lambda$ , the Ly $\beta$  and Ly $\gamma$  troughs are even more sensitive than Ly $\alpha$  to the start of reionization.

transition	wavelength	$f_{lu}$
Ly $\alpha$	1215.67	.4162
Ly $\beta$	1025.72	.07910
Ly $\gamma$	972.54	0.02899

- Consideration of the first ionizing stars (to be discussed in Lec28) leads to the idea that their HII regions grow and multiply, and merge, producing a clumpy universe.
- The development of the GP near  $z \sim 6$  involves both an increase in the density of Ly $\alpha$  forest lines but also the diminution of the ionizing flux.

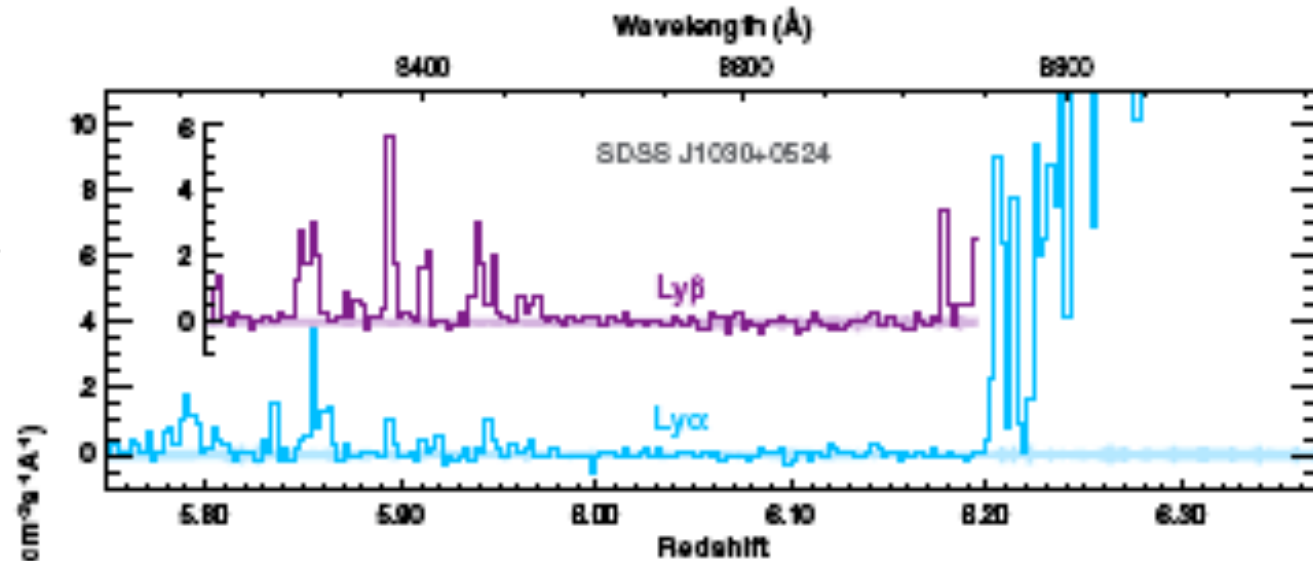
# Growth of the GP Trough Towards $z = 6.42$



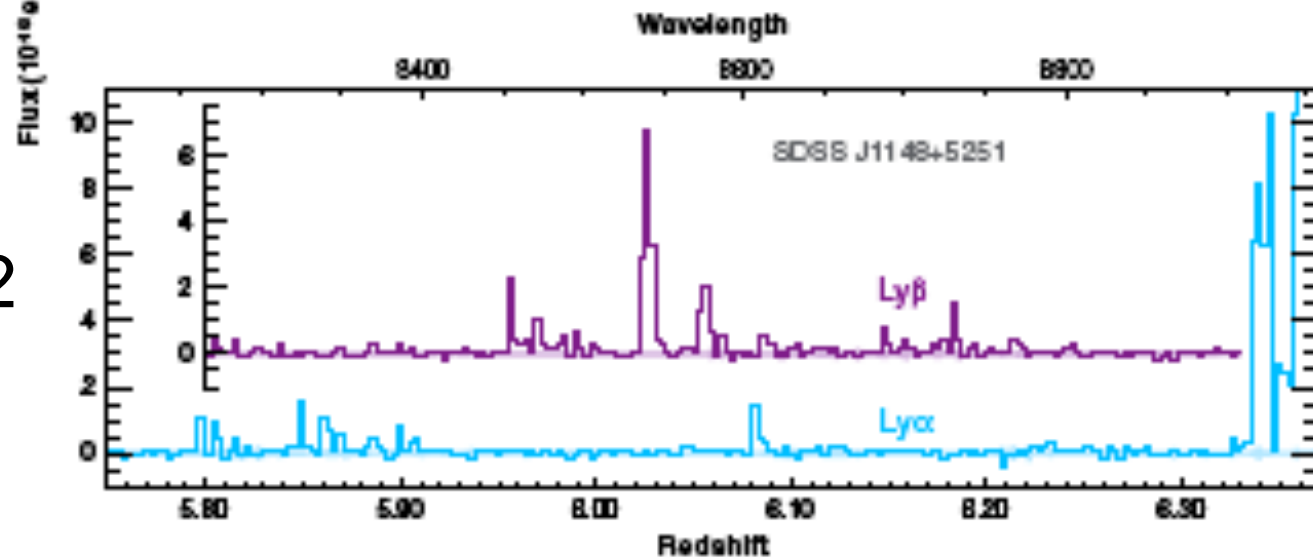
Detailed examination of GP troughs indicates that  $\tau_{\text{GP}}$  varies with direction, suggestive of variations in the re-ionizing radiation.

# Troughs for the Two Highest-z Quasars

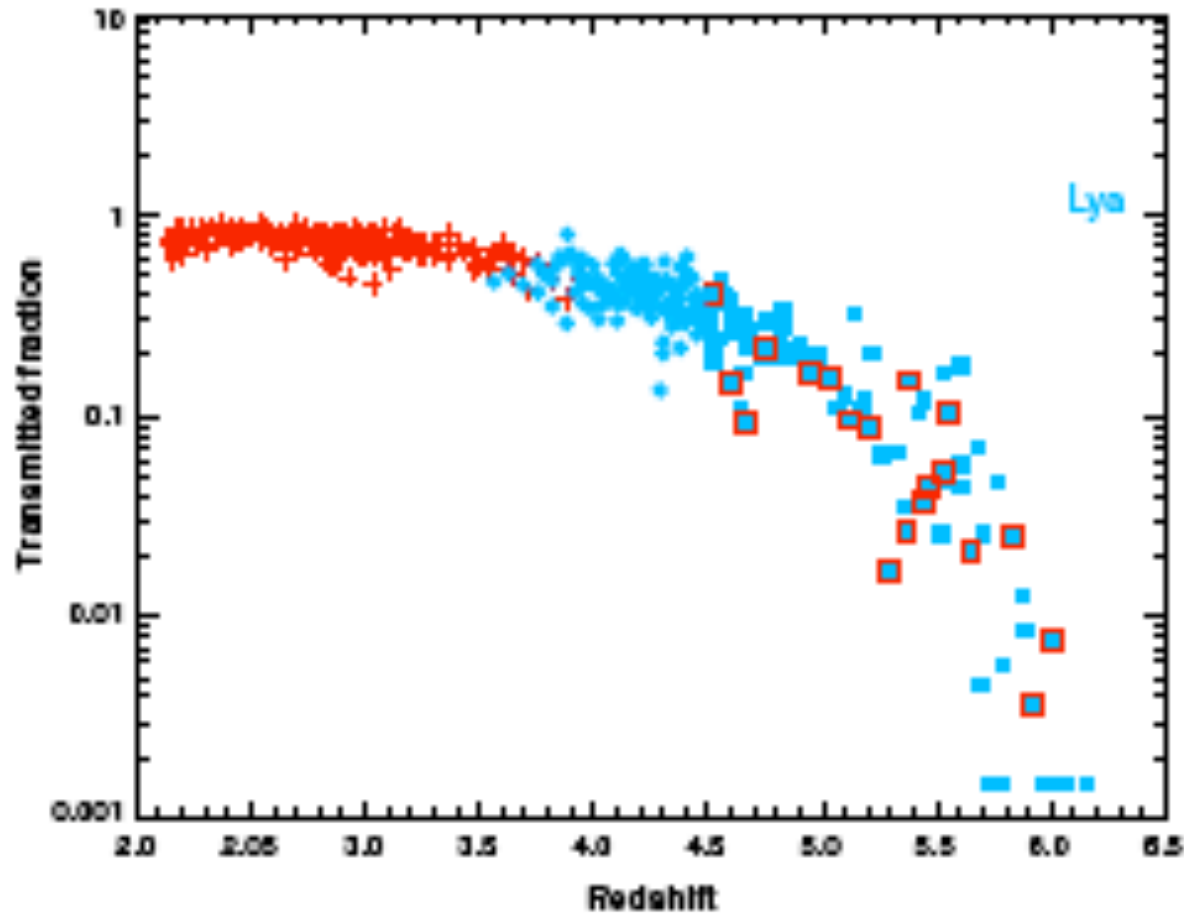
$z = 6.28$



$z = 6.42$



# Transmitted Flux in the GP Trough



Tiny fluxes for  $z \rightarrow 6$   
Songaila AJ 127 2598 2004

# Increase of GP Optical Depth With $z$

Fan et al. AJ 132 117 2006

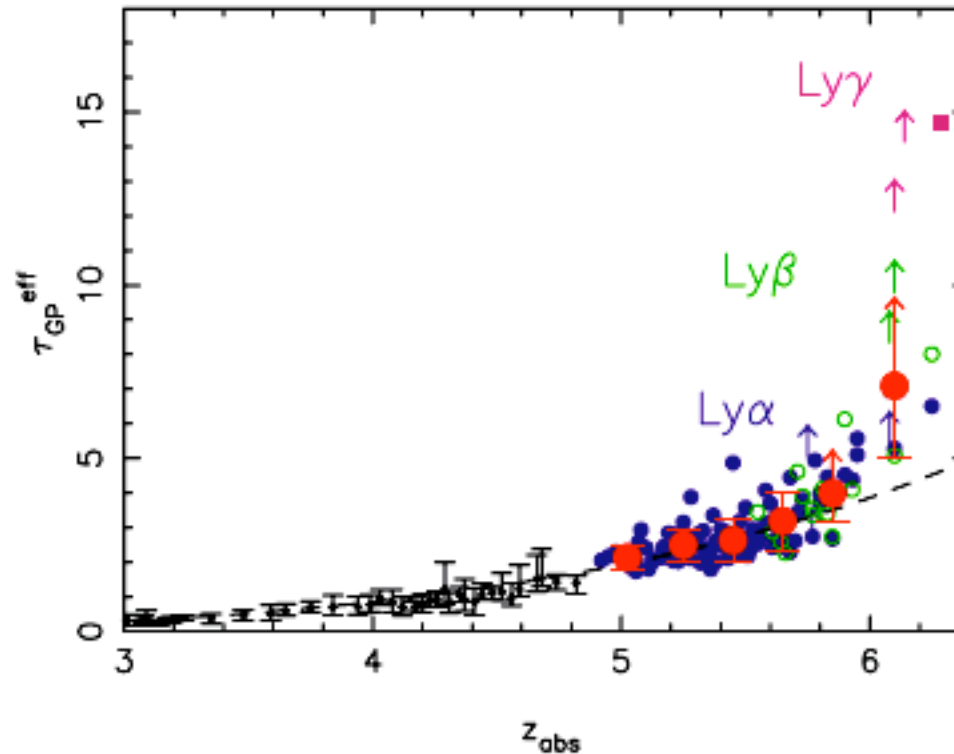
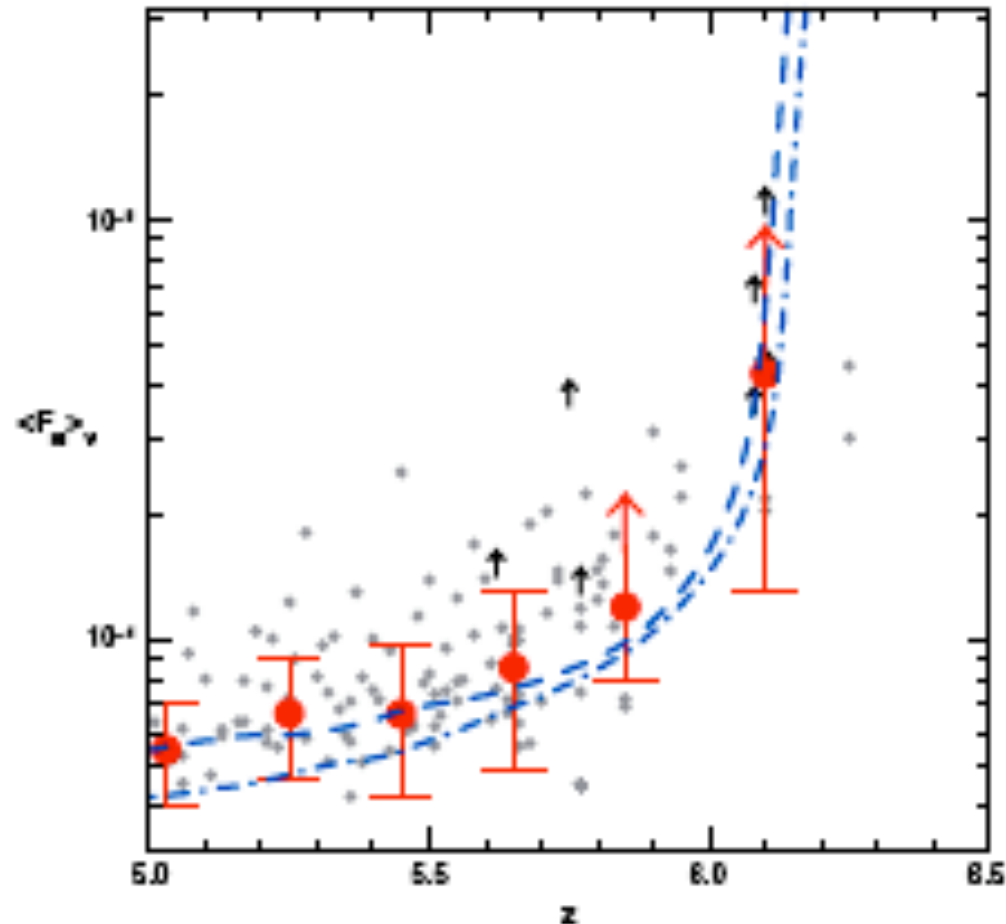


FIG. 5.—Evolution of optical depth combined with the Ly $\alpha$ , Ly $\beta$ , and Ly $\gamma$  results. The Ly $\beta$  measurements are converted to Ly $\alpha$  GP optical depth using a conversion factor of 2.25. The values in the two highest redshift bins are lower limits, since they both contain complete GP troughs. The dashed line shows a redshift evolution of  $\tau_{\text{GP}}^{\text{eff}} \propto (1+z)^{4.3}$ . At  $z > 5.5$ , the best-fit evolution has  $\tau_{\text{GP}}^{\text{eff}} \propto (1+z)^{10.9}$ , indicating an accelerated evolution. The large filled symbols with error bars are the average and standard deviation of optical depth at each redshift. The sample variance also increases rapidly with redshift. We also include the Ly $\gamma$  measurements (*square*, Table 4); they cover only the high-redshift end of the Ly $\alpha$  and Ly $\beta$  bins due to contamination from Ly $\delta$  absorption along the line of sight at lower redshift.

# HI Fraction for 19 High-z Quasars

Fan et al. AJ 132 117 2006



Lower limits to the HI fraction for  $z = 5.0 - 6.2$   
Based on models of the ionizing radiation  
(dashed lines are numerical simulations)

## 5. Reionization of He II

Basic facts about He II:

$$\begin{aligned} \text{IP} &= 54.418 \text{ eV} & (227.8 \text{ \AA}) \\ E(\text{Ly}\alpha) &= 40.81 \text{ eV} & (303.8 \text{ \AA}) \end{aligned}$$

which imply:

1. Much harder UV radiation is needed to ionize He II than H I (maybe quasars rather than stars).
2. Detecting He II in high- $z$  quasars requires UV observations, e.g., for HeII Ly  $\alpha$  is shifted to  $1215\text{\AA}$  for  $z = 3$ .
3. HST has UV capability down to  $1150 \text{ \AA}$  and FUSE provides high resolution from  $905\text{-}1195 \text{ \AA}$ .
4. Five examples known (as of 2005)

*He II Ly  $\alpha$  observations provides unique information about the spectrum of ionizing radiation in the IGM.*



# He II in the IGM With FUSE

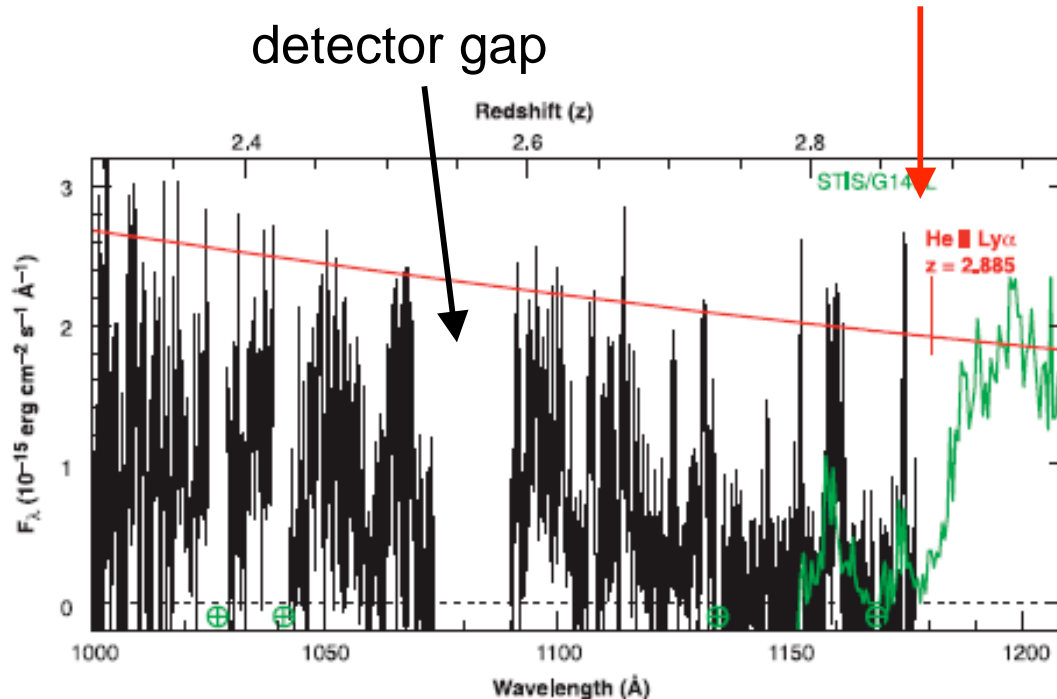


Fig. 1. FUSE spectrum of HE2347-4342 (binned to 0.05 Å pixels) is shown in black. Bins at the peak fluxes have a signal-to-noise ratio of  $\sim 7$ . A portion of the contemporaneous STIS spectrum is shown in green. The red line is the extrapolation of the power law plus extinction of  $E(B - V) = 0.014$  fitted to the STIS spectrum. The position of He II Ly $\alpha$  at the redshift of HE2347-4342 is marked. Gaps in the FUSE spectrum due to excised terrestrial airglow lines are marked with green  $\oplus$ . The broad gap from 1072 to 1089 Å is due to gaps between the FUSE detector segments.

Q 2347-4342

$z = 2.885$

Green: HST STIS spectrum

Red: extrapolated STIS  
continuum

**He II reionization  
occurred near  
 $z = 3$ , i.e. later than  
H reionization**

Kriss et al. Science, 293 1112 2001 (FUSE + STIS)

See Zheng et al. ApJ 2004 (FUSE + VLT) for a *re-*

*analysis* of He II Ly clouds in the spectrum of this quasar.